Earth, Planets and Space

EXPRESS LETTER Open Access

Seasonal variation of inter-hemispheric field-aligned currents deduced from time-series analysis of the equatorial geomagnetic field data during solar cycle 23–24

Manjula Ranasinghe[1], Akiko Fujimoto[2*], Akimasa Yoshikawa[3] and Chandana Jayaratne[1]

Abstract

The east–west component of magnetic field variation (ΔD-component) at Davao station (Philippines, geomagnetic latitude: – 2.22˚N) are used to investigate the characteristics of the long-term Inter-Hemispheric Field-Aligned Currents (IHFACs) based on the time-series analysis from August 1998 to July 2020. Recent in situ satellite and ground-based observations have reported that dusk-side current polarity of IHFAC is often opposite to that of the noon IHFAC, being inconsistent with Fukushima's IHFACs model. We investigated the consistency of the dusk-side IHFAC polarity derived from the observations with the polarity expected from Fukushima's IHFACs model and examined the solar cycle dependence of IHFACs. It was confirmed that the dusk-side IHFACs during June and December solstices flow in the same direction of the noontime IHFACs, which was consistent with the IHFAC polarities suggested by the Fukushima model. The dusk-side IHFACs around March and September–November months disagreed with the Fukushima model. The ΔD variations clearly showed seasonal asymmetry in the dawn and noon sectors, whereas the ΔD variations in the dusk sector demonstrated seasonal symmetry. Solar cycle dependence of IHFACs was exhibited in the dusk sector. For the dawn and noon sectors, the yearly peak-to-peak ΔD amplitude in the later solar cycle SC24 decreased by about 35% in comparison with the earlier solar cycle SC23. In contrast, the dusk-side yearly peak-to-peak ΔD amplitude increased by about 200%. The dusk-side IHFAC yearly amplitude tended to be in inverse proportion to solar activity.

Keywords: Inter-hemispheric field-aligned currents (IHFACs), Ground-based magnetometer data, Equatorial magnetic field, Solar cycle SC23 and SC24, MAGDAS/CPMN, Seasonal variations, Fukushima's model

Introduction

The Inter-Hemispheric Field-Aligned Current (IHFAC) is one of the major current systems causing changes in the geomagnetic field at low and middle latitudes. IHFACs flow from the summer hemisphere to the winter hemisphere in the dawn sector and from the winter hemisphere to the summer hemisphere in the noon and dusk sectors (Fukushima, 1994). Van Sabben (1966) first suggested the existence of IHFACs by using the north–south difference of equivalent Sq current. The IHFACs are caused by the inter-hemispheric imbalance of the ionospheric solar quiet (Sq) current system at the middle–low latitudes (Van Sabben 1966, 1969, 1970), due to asymmetry of the north–south Sq current vortices that establishes a potential difference between the northern and southern hemispheres (Fukushima, 1979; Tomás et al. 2009). Many numerical calculation studies have predicted IHFAC intensity and supported the dependence of IHFAC current polarity changing with local time (Maeda

*Correspondence: fujimoto@ai.kyutech.ac.jp
[2] Faculty of Computer Science and Systems Engineering, Kyushu Institute of Technology, 680-4, Kawazu, Iizuka, Fukuoka 820-8502, Japan
Full list of author information is available at the end of the article

1974; Schieldge et al. 1973; Stening 1977; Takeda 1982; Van Sabben 1969, 1970).

Fukushima's IHFAC model is characterized by the following features: (1) IHFACs flow from the summer hemisphere to the winter hemisphere in the dawn sector and the opposite current flows in the noon sector; (2) IHFACs polarity between the noon and dusk sectors is in-phase and (3) the absolute intensity of IHFACs is stronger in both dawn and noon sectors than the dusk sector. The current polarity of Fukushima's IHFACs model has been supported by in situ satellite observations and ground-based magnetometer data analysis as well as the above-mentioned numerical studies. The first experimental evidence has been provided from Magsat observations (Olsen 1997). The characteristics of IHFACs have been extensively described by many papers, for example, seasonal climatology of IHFACs by the Ørsted satellite (Yamashita and Iyemori 2002), seasonal, longitudinal, and local-time IHFACs variations by the CHAMP satellite (Park et al. 2011) and the Swarm satellite constellation (Lühr et al. 2015, 2019; Fathy et al. 2019; Park et al. 2020b), ground-based local-time and seasonal dependence (Bolaji et al. 2012; Shinbori et al. 2017; Abidin et al. 2019) and latitudinal dependence (Owolabi et al. 2018).

In recent years, the IHFACs characteristics in the dusk sector, which disagrees with the concept of the Fukushima's model, have been reported by ground-based magnetometer (Shinbori et al. 2017) and satellite observations (Lühr et al. 2015, 2019; Fathy et al. 2019; Park et al. 2011, 2020a, 2020b). These papers show the dusk-side IHFACs flowing southbound irrespective of season, by using the average value of magnetic field obtained from in situ satellite or ground-based magnetometer observations for each month in 1-h local time (LT) bin. Although these analyses revealed the average distribution of IHFAC polarity, little attention has been paid to the relationship of IHFAC polarities between the noon and dusk sectors for individual days. In addition, their analysis periods were almost too limited to demonstrate the solar cycle dependence of IHFACs, namely less than solar cycle period (11 years) (e.g., Park et al. 2011; Owolabi et al. 2018; Lühr et al. 2019). Shinbori et al. (2017) used long-term (59 years) ground-based magnetometer data for the comparison of IHFAC intensity between higher and lower solar activity periods. They examined the monthly average of IHFAC variations, but disregarded to compare the IHFAC polarities in the noon and dusk sectors for individual days. It is essential to investigate the occurrence rate of the dusk-side IHFAC suggested by the Fukushima's model (hereafter, the dusk-side IHFACs of the Fukushima's model type), in order to conclude the consistency between the dusk-side IHFAC polarity derived from the observations and the IHFAC polarity expected from the Fukushima model.

In order to discuss the presence of the dusk-side IHFACs of the Fukushima model type, it is important to conduct a long-term time-series analysis of IHFAC variations, in terms of the comparison of IHFACs polarities between noon and dusk sectors for individual days. In contrast to the in situ satellite observations which provide the global distribution of IHFACs two-dimensional map (longitude–latitude), the ground-based magnetometer data allows us to investigate the daily IHFAC variations. In other words, the in situ observations cannot provide the comparison of IHFAC variations of each LT of a single day, but the ground-based observations enable us to analyze the relationship of IHFAC polarity among the different LT for individual days. The equatorial *D*-component magnetic fields are used in this paper, since they include more essential effects of IHFAC variation than the equatorial *H*-component magnetic fields which are dominated by the equatorial electrojet effect (Yamazaki and Maute, 2017).

Field-aligned currents (FACs) observed at the high-latitude regions are excited by the plasma environment and its dynamics in the magnetosphere. Their existence strongly reflects the interaction between the solar wind, magnetosphere, and ionosphere. On the other hand, the IHFAC, which we focus on in this paper, is a current system flowing along the magnetic field line that is excited by reflecting the asymmetry of ionospheric current system between the northern and southern hemispheres. At low and middle latitudes, electromotive forces generating ionospheric currents act as a dynamo caused by the atmospheric wind and the penetrated electric field from the polar to equatorial ionosphere which involves a variety of ranges of spatiotemporal phenomena. Therefore, a close examination of IHFACs is very important for understanding the magnetosphere–ionosphere coupling system excited by the solar wind, the global atmospheric motion driven by sunlight, and the electromagnetic environment of the global near-earth system resulting from their coupling.

Although most of the earlier studies have confirmed the existence of IHFACs, few explanations have fully proposed for the characteristics of dusk-side IHFAC based on the ground-based observational data in terms of the time-series analysis. Since IHFACs are excited along the magnetic field lines at middle and low latitudes, their development is known to be remarkably apparent in the east–west component of the ground magnetic field data. This study aims to understand the long-term variation of the IHFAC using the east–west component of the low-latitude geomagnetic field data continuously observed for

two solar cycles, and to develop the leading edge of systematic IHFAC research.

The main purpose of this paper is to investigate the relationship between noon and dusk of IHFAC polarity for individual days, by using long-term ground-based equatorial magnetometer data from 1998 to 2020. The present study focuses on analyzing the occurrence rate of the dusk-side IHFAC of the Fukushima model type. Namely, we calculate the ratio of the number of days having the same polarity between the noon and dusk sectors to the total number of observational days. In addition, we examine the time-series data of IHFACs for monitoring of the solar cycle dependence of IHFACs. The analysis of the 22-year long-term data enables us to investigate the solar cycle dependence of IHFACs (Fujimoto et al. 2016), which is the secondary purpose of this work. In the following, the section "Observation data and analysis method" briefly describes the observational data, their sources, and data analysis method to determine the variation of IHFACs (ΔD magnetic field variations). The section "Results and discussion" demonstrates and discusses characteristics of the long-term ΔD variations, the occurrence rate of the dusk-side IHFACs of the Fukushima model type, and climatology of IHFACs polarity in terms of solar cycle dependence of IHFACs. The section "Conclusion" summarizes the present study.

Observation data and analysis method

We used long-term MAGnetic Data Acquisition System/Circum-pan Pacific Magnetometer Network Data (MAGDAS/CPMN) magnetometer 1-h time resolution data at Davao station (Geographical latitude 7˚N, Geographical longitude 124.5˚E, Geomagnetic latitude − 2.22˚N, Geomagnetic longitude 197.9˚E, Dip latitude − 0.24˚) operated by International Center for Space Weather Science and Education (ICSWSE), Kyushu University (Yumoto et al. 1996, 2001, 2006, 2007), from 1998 August to 2020 July. The *D*-component (the east–west component) of magnetic field was analyzed for investigating the characteristics of IHFACs, since the northward and southward IHFACs induce the westward and eastward magnetic field variations on the ground, respectively. Since the geomagnetic field at Davao is approximately horizontal on the magnetic equator (Davao station is located near at the magnetic equator), we assume that the *D*-component is due to the magnetic field variation caused by IHFACs. In this paper, "northward IHFACs" is referred as the current flowing from the southern hemisphere to northern hemisphere. The westward ΔD magnetic field corresponds to the northward IHFACs, whereas the eastward ΔD magnetic field corresponds to the southward IHFACs.

To derive the IHFACs effect from the *D*-component variation, we first subtracted the base line calculated by using the midnight averaged values from each hour data point. Since the source of the daytime ionospheric wind dynamo is the solar daily radiations, the magnetic effect of this dynamo is generally negligible during the nighttime (Yamazaki and Maute 2017). Fambitakoye and Mayaud (1976) determined the base level by interpolating linearly between two midnights neighboring the day considered. This derivation manner was adapted in this paper.

The daily variation of the *D*-component, ΔD, was calculated with respect to the midnight-to-midnight baseline (daily baseline). Midnight data points for the daily baseline were selected as hourly values of previous day 23:00 LT (D_{p23h}, the subscript "p" indicates "previous"), previous midnight 00:00 LT (D_{p00h}), target day 01:00 LT (D_{00h}), target day 23:00 LT (D_{23h}), next midnight 00:00 LT (D_{n00h}, the subscript "n" indicates "next") and next day 01:00 LT (D_{n01h}). The baseline was calculated as a linear function which fits for these six data points near midnight. The linear function is represented as the following Eq. (1) and slope a and y-intercept b are constants to be determined.

$$y = ax + b. \tag{1}$$

Domain values for x (D_{p23h}, D_{p00h}, D_{00h}, D_{23h}, D_{n00h}, and D_{n01h}) were determined as (−1, 0, 1, 23, 24, and 25) according to the following function (2) so that the distance between x values of any adjacent hours becomes one and the distance between any x values gives the number of hours between those data points:

$$f_x(h) = \begin{cases} h - 24, & \text{if hour } h \text{ in previous day, } \{h|h = 23\} \\ h, & \text{if hour } h \text{ in target day, } \{h|\, h = 0, 1, 23\} \\ h + 24, & \text{if hour } h \text{ in next day, } \{h|h = 0,\ 1\} \end{cases} \tag{2}$$

The linear function constants a and b were calculated using the least squares polynomial fit technique so that the calculated linear function can be as representative as possible of all data points. The projected data points of the daily base line for any given hour were calculated according to the following Eq. (3):

$$D_b(h) = ah + b, \{h \in \mathbb{Z} | -1 \le h \le 25\}. \tag{3}$$

ΔD represents the daily variation of the *D*-component relative to the daily base line, calculating for each day as below:

$$\Delta D_h = D_h - D_b(h), \{h \in \mathbb{Z} | 0 \le h \le 23\}. \tag{4}$$

F10.7 cm Radio Flux index (F10.7) and *Dst* index were used to monitor the solar cycle activity and the magnetospheric disturbances, respectively. Daily F10.7 and *Dst*

index data were obtained from SPDF OMNIWeb (King and Papitashvili 2005; SPDF-OMNIWeb Service 2020). The original source of *Dst* is WDC geomagnetism Kyoto. The analysis period from 1998 to 2020 includes most of the latest two solar cycles SC23 (1996–2008) and SC24 (2008–2019, NASA officially announced that SC25 has begun in 2019 December [NASA 2020]).

Results and discussion

Characteristics of IHFACs in the dusk sector

We examined ΔD variations to demonstrate the transition of IHFAC polarity, especially the dusk-side IHFAC polarity change against the noontime IHFAC polarity. Figure 1 shows examples of ΔD variations as a function of local time (LT) and day of year, in 2010, 2013, 2015 and 2016. These years were selected to show the following typical patterns in different solar activity periods in SC24. The directions of IHFACs among both hemispheres reversed twice around the months of February and October, but not exactly during the March and September equinoxes. During the March–September months, the eastward ΔD (=southward IHFACs) and the westward ΔD (=northward IHFACs) were observed in the dawn (06–08 h, LT) and noon (11–13 h, LT) sectors, respectively. For these two sectors, the directions of IHFACs during October–February months were opposite to those of March–September months. The dusk (16–18 h, LT) IHFACs around June and December solstices had roughly the same polarity as the noon sector. The reversal of IHFAC polarity between the noon and dusk sectors frequently occurred in all months except for the June and December months. We found this tendency in all years analyzed in this paper (1998–2020).

In order to clarify the occurrence rate of the dusk-side IHFAC of the Fukushima model type, we calculated the ratio of the number of days having the same polarity between the noon and dusk sectors to the total number of observational days, for each month in each year bin (Fig. 2a). As shown in Fig. 2a, high occurrences of the dusk-side IHFAC of the Fukushima model type appeared around June and December solstices and the occurrence rate was low during the March–April and September–November months (Fig. 2b). The results indicate that there is a seasonal dependence of the dusk-side IHFAC of the Fukushima model type.

For the dusk-side IHFAC polarity, the earlier studies based on in situ and ground-based observations have shown the consistency of the Fukushima model (Olsen 1997; Yamashita and Iyemori 2002), whereas some recent in situ and ground-based observational studies claimed the opposite direction of dusk-side IHFACs (Lühr et al. 2015, 2019; Fathy et al. 2019; Park et al. 2011, 2020a, 2020b; Shinbori et al. 2017). These previous studies have analyzed the monthly, seasonal (combining 2–3 months)

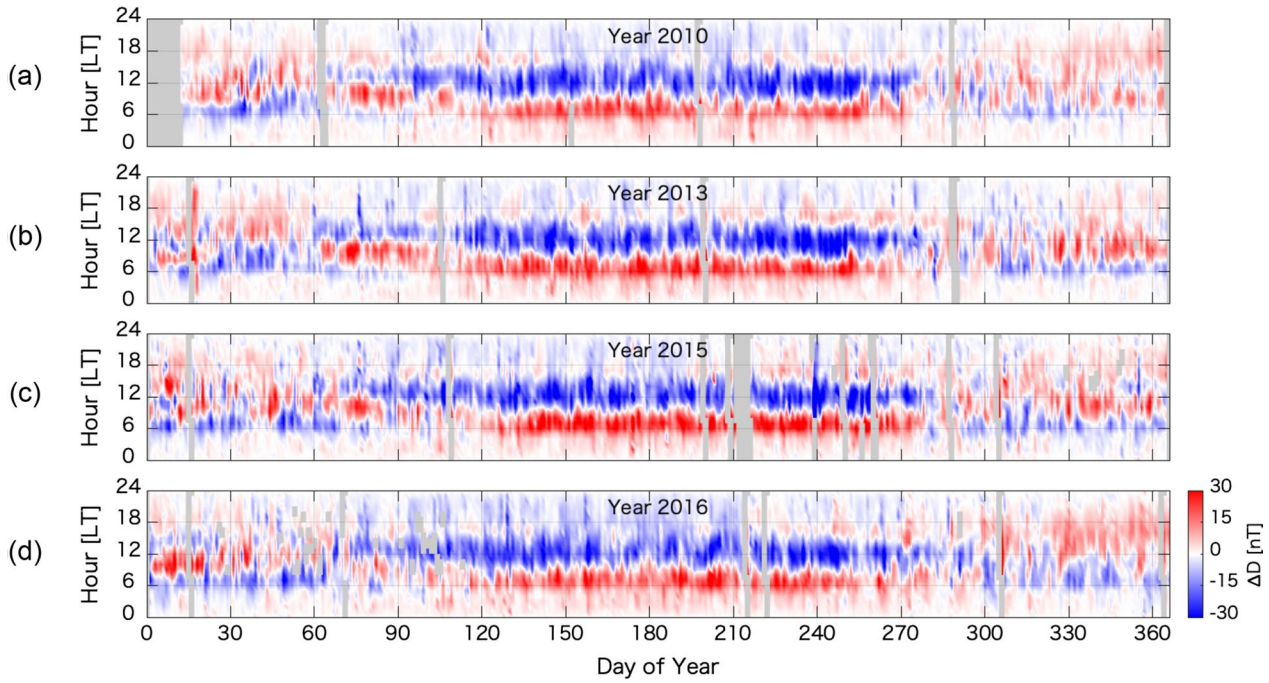

Fig. 1 Daily ΔD variations at Davao as a function of local time and day of year. **a** 2010, **b** 2013, **c** 2015, **d** 2016. The color bar shows the intensity of ΔD. The red (=eastward ΔD) and blue (=westward ΔD) colors correspond to the southward IHFACs and the northward IHFACs, respectively

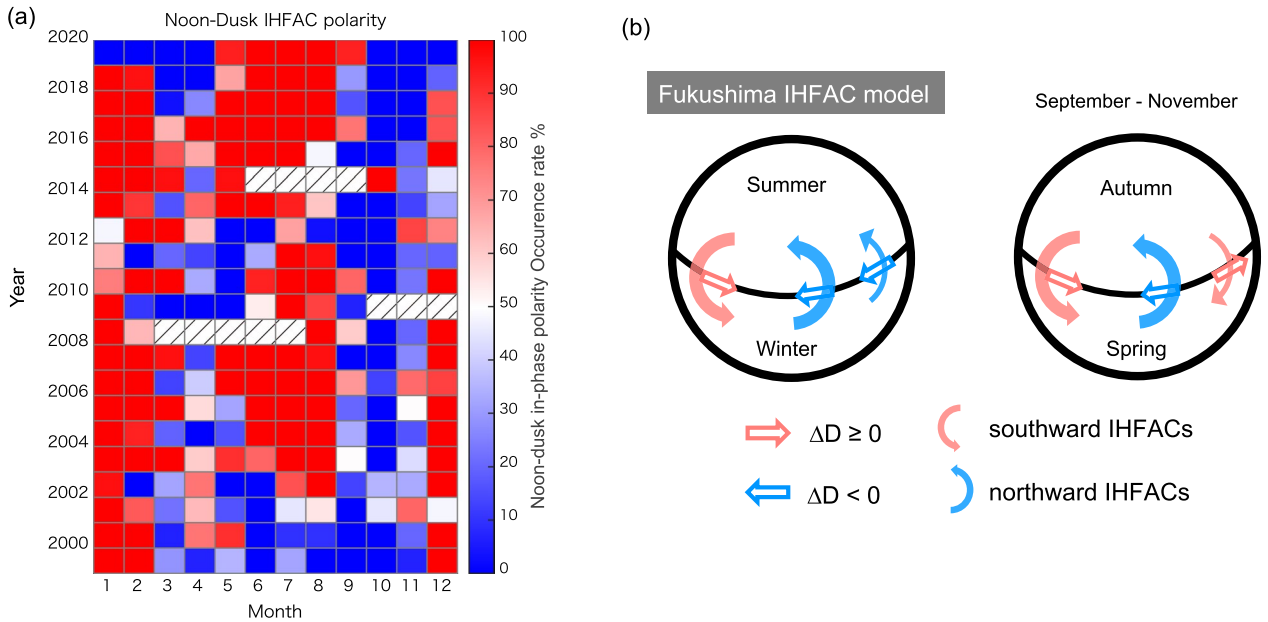

Fig. 2 Distribution of the dusk-side IHFAC of the Fukushima's model type from 1999 to 2019. **a** The occurrence rate of the dusk-side IHFAC of the Fukushima's model type as a function of month and year. The red color indicates higher occurrence of the dusk-side IHFAC of the Fukushima's model type, which means the in-phase IHFAC polarity in both noon and dusk sectors. The blue color represents lower occurrence rate, this is equal to higher occurrences of the dusk-side IHFAC, which disagreed with the concept of Fukushima's model. The hatched areas show the no-data periods. **b** The illustration of IHFACs polarity. The left side describes the concept of Fukushima's model for the northern hemisphere in summer. The right side shows the opposite dusk-side IHFAC of the Fukushima's model type

or several-year average values of IHFACs in each LT sector. These approaches, however, have not examined the relationship between the noon and dusk IHFAC polarity for individual days. Consequently, although many studies have been conducted using in situ and ground-based observations, there is little agreement on the dusk-side IHFAC polarity as suggested by Fukushima (1979, 1994). The occurrence rate of the dusk-side IHFAC of the Fukushima model type is examined by this work for the first time, and our findings reveal the seasonal dependence of occurrence distributions of the dusk-side IHFAC polarity over the long term.

Figure 3 shows solar cycle dependences of ΔD variations. Figure 3a is the sample plot of monthly averaged of ΔD variations in the dawn sector in 2019. The dawn-side IHFAC polarity flows northbound from November to April and the southward IHFAC occurs from May to October. Figure 3b shows the monthly average value of ΔD for each LT sector and solar cycle activity phase, indicating remarkable asymmetry in seasonal IHFACs variation in both the dawn and noon sectors. Absolute monthly averaged ΔD values in both the dawn and noon sectors were stronger around the September equinox, $|\Delta D| \sim 30$ nT, and weaker around the December solstice, $|\Delta D| \sim 10$ nT. The dawn-side and noontime ΔD variations exhibited a remarkable seasonal asymmetry. On the other hand, the dusk-side ΔD variations showed symmetry throughout year, with $|\Delta D| \sim 5$ nT. Our result of monthly averaged ΔD variations at Davao agrees with the result at Guam presented by Shinbori et al. (2017), but there are weak seasonal asymmetries in dawn and noon sectors at Guam. The asymmetry pattern of ΔD, however, is clearly seen in our result. The magnetic field fluctuations caused by IHFACs could be detected effectively in ΔD variations at Davao, because the Davao station is located nearer to the magnetic equator than the Guam station. The IHFAC model proposed in Fukushima [1979] originates from the summer–winter hemisphere asymmetry of the Sq current system caused by the neutral wind dynamo. Yamazaki et al. (2011) showed that seasonal variations of the equivalent Sq current intensity reproduced from the 210 MM magnetometer chain exhibit north–south asymmetry. The equivalent Sq current in the northern summer has a stronger intensity than that in the southern summer. Since the source of the IHFACs is the north–south asymmetry of Sq current, the seasonal north–south asymmetry of Sq current could cause the asymmetry in seasonal monthly averaged ΔD variations.

Our results show that the dusk-side IHFAC polarity during June and December solstices agreed with the polarity proposed by the Fukushima model, whereas the dusk-side IHFAC polarity disagreed during equinoxes.

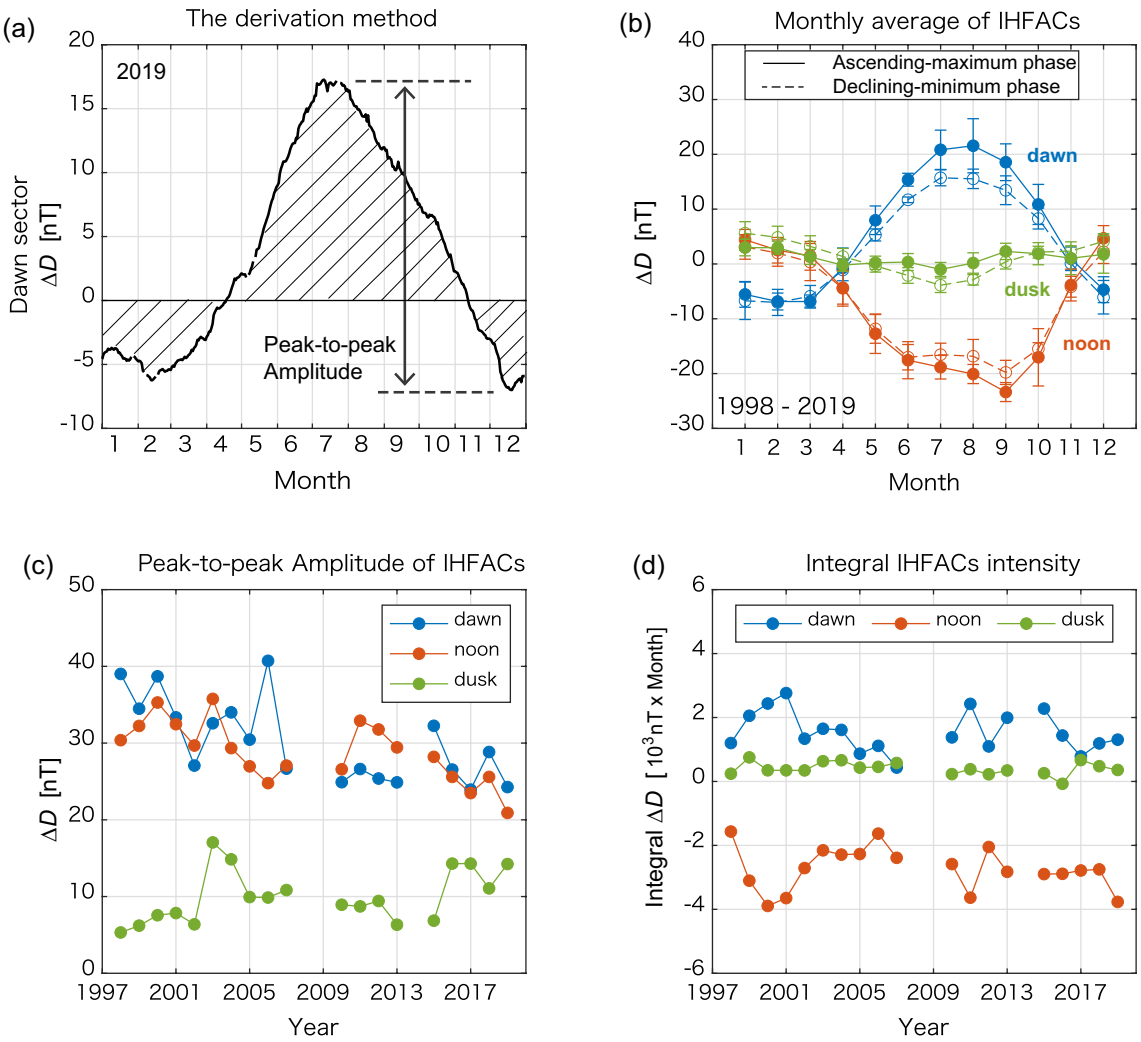

Fig. 3 Solar cycle dependence of Δ*D* variations. **a** Illustration of the derivation method of peak-to-peak amplitude and integral intensity of Δ*D* variations; **b** monthly average of Δ*D* variations plotted by the separated groups in terms of solar cycle activity: the ascending-maximum phase (1998–2003, 2011–2015) as shown with solid lines and declining-minimum phase (2004–2010, 2016–2019) as indicated by dashed lines, the error bar shows standard deviations for each data point. **c** Peak-to-peak amplitude of yearly Δ*D* variations; **d** yearly integral intensity of Δ*D* variations, which is provided by the summation of hatched areas in panel (**a**). Through (**b**–**d**), the blue, red and green colors represent the dawn, noon and dusk sectors, respectively. The data points for 2008, 2009, and 2014 were removed due to the lack of data per year

What is a cause of the dusk-side IHFAC flowing the opposite direction of noontime IHFAC? The period of the dusk-side IHFAC with the opposite polarity of the Fukushima model corresponds to the transition phase when the direction of IHFACs reverses among both hemispheres. Figure 3b presents additional information regarding the month of intersection where IHFACs reversed. For the dusk sector, the intersection months were April and September. The noontime intersections were March and November. It is clear that the noontime and dusk-side IHFACs reversed at the different months. There are known seasonal and solar cycle variabilities of the high-latitude current system, and parts of this system are also highly dependent on external driving such as solar wind conditions (Green et al. 2009; Ridley 2007; Edwards et al. 2017; Christiansen et al. 2002). Considering the above-mentioned different reversal month of the IHFAC polarity, we speculate that the appearance pattern of dusk-side IHFAC results from the present analysis could originate from the superposition of the global current system extending from the polar region. In order to investigate this scenario, it is necessary to proceed with comparative analysis between the long-term development of the global current system from the polar to

middle and low latitudes and the IHFACs excitation pattern. A further analysis of this point should be conducted.

Solar cycle dependence of IHFACs

In this subsection, we focus on the climatology of IHFACs polarity variation. Thus, the daily IHFAC polarity variations are ignored, and the analysis and discussion are limited to seasonal and solar cycle variation. We applied the 61-day centered moving average to ΔD variations with respect to each local time, in order to monitor the long-term transition of IHFAC polarity. The reason why the smoothing value (=61 days) was selected is because we wanted to disregard variations with frequencies higher than two months. Figure 4 shows the long-term transition of IHFAC polarity from 1999 to 2019 with F10.7 and *Dst* index. We found that annual cyclic variations of ΔD in the dawn and noon sectors and multiple periodicities in the dusk sector. Figure 4b–d

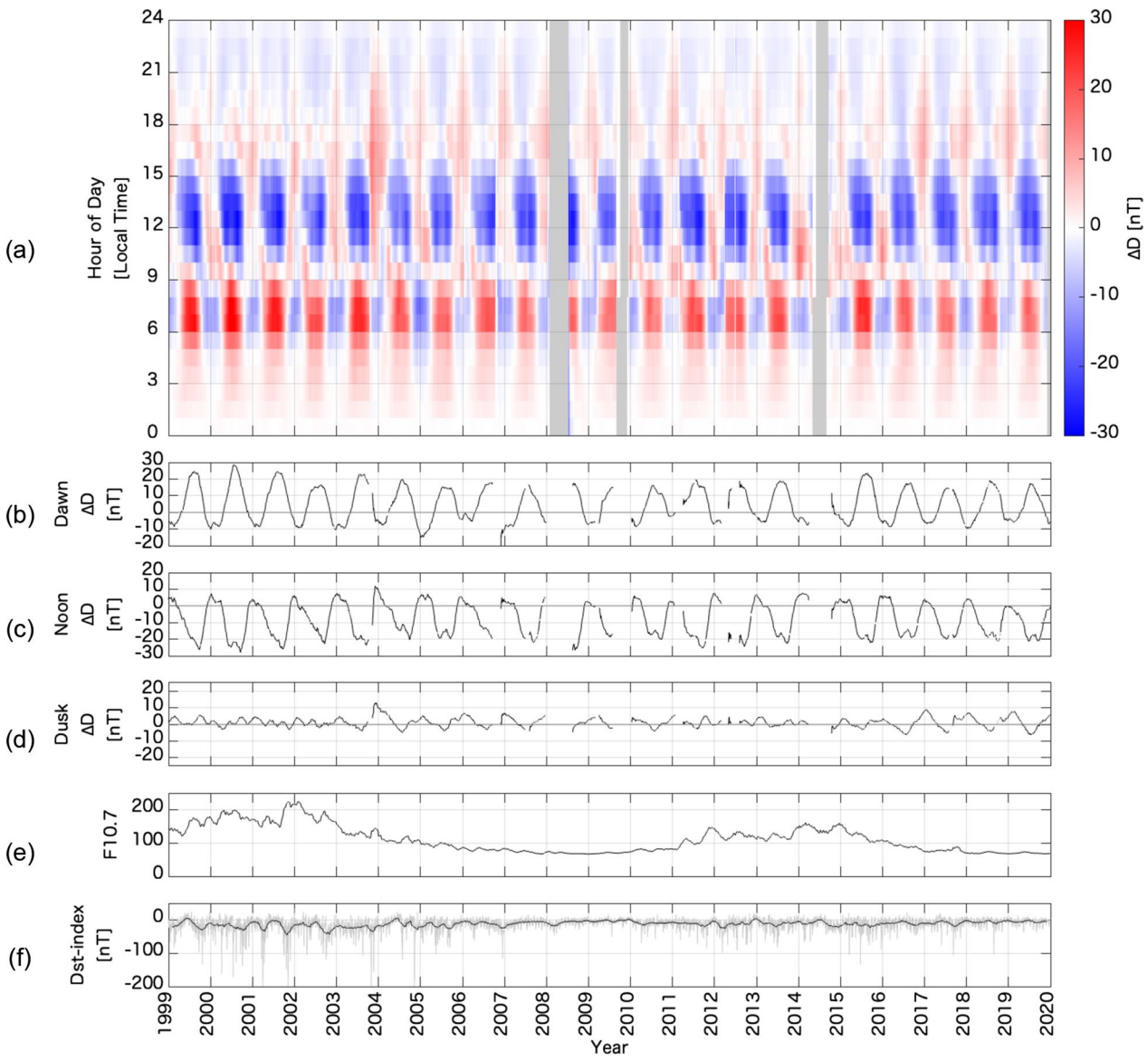

Fig. 4 Long-term ΔD variation with F10.7 and *Dst* index, from 1999 to 2019. a 61-day centered moving-averaged ΔD respect to each local time (LT), gray shade patch indicates the lack of data; b 61-day centered moving-averaged ΔD in dawn sector (06–08 h, LT); c 61-day centered moving-averaged ΔD in noon sector (11–13 h, LT); d 61-day centered moving-averaged ΔD in dusk sector (16–18 h, LT); e 61-day centered moving-averaged daily F10.7 index; f daily *Dst* index and 61-day centered moving-averaged daily *Dst* index are plotted with gray and black solid lines, respectively

shows the time-series data of ΔD variations in each LT sector (dawn, noon, and dusk). We can see that the relationship of ΔD variations between the dawn and noon sectors is out-of-phase ~ 180˚. As shown in Fig. 4d, the dusk-side IHFAC polarity has an annual variation during the declining phase of the solar cycle and semiannual or terannual variations during the solar cycle's ascending-maximum phase.

As shown in Fig. 3b, the monthly averaged ΔD variations were classified into two groups in terms of solar cycle activity: the ascending-maximum phase (1998–2003, 2011–2015) and declining-minimum phase (2004–2010, 2016–2019). For the dawn and noon sectors, the absolute monthly averaged ΔD values were larger during the ascending-maximum phase than those during the declining-minimum phase. This result is consistent with the result from the ground-based equatorial magnetometer observations by Shinbori et al. (2017). The features of the dawn and noon sectors in Fig. 3b show an asymmetry that tracks with season, regardless of the solar cycle. The yearly integral intensity of ΔD was calculated to examine the total amount of IHFACs in regards to solar cycle activity (Fig. 3d). The yearly integral intensity of ΔD was derived by the summation of ΔD (hatched areas in Fig. 3a) for each year.

We derived the peak-to-peak amplitude of yearly ΔD in each LT sectors to discuss the solar cycle dependence of yearly IHFACs (Fig. 3c). The peak-to-peak amplitude of yearly ΔD in each sector was defined by the difference between the maximum and minimum of monthly averages of the daily averaged IHFAC values per each year (the derivation method, Fig. 3a). As shown in Fig. 3c, the peak-to-peak amplitude values of yearly ΔD were roughly 2–3 times larger in the dawn and noon sectors than that in the dusk sector. The peak-to-peak amplitude values decreased with increasing year in the dawn and noon sectors, whereas the trend of peak-to-peak amplitude in the dusk sector increased slightly over the long term. This is the opposite trend of the yearly peak-to-peak amplitude in dawn-side and noontime. The variation ratio of peak-to-peak amplitude IHFAC for each LT sector was estimated according to the following equation, $(\Delta D_{2019} - \Delta D_{1998})/\Delta D_{1998}$. For the dawn and noon sectors, the yearly ΔD amplitude in the later solar cycle SC24 decreased by about 35% in comparison with the earlier solar cycle. In contrast, the yearly dusk-side ΔD amplitude increased by about 200%. Along with the slight overall increase from 1998 to 2019, we see larger yearly amplitudes of dusk IHFACs during the declining phases of both solar cycles (2003–2007, and 2016–2019) than during other phases. Concerning the effect from the magnetosphere, for example, the dusk-side ΔD could be disturbed by the partial ring current caused by geomagnetic storms. Especially, the declining phase has been shown to produce different kinds of solar wind driving conditions than what happens during solar maximum (e.g., Richardson et al. 2001; Echer et al. 2008; Webb 1995), which can result in different behaviors in the magnetospheric storm-time response, such as the duration and intensity of the storm (e.g., Borovsky and Denton 2006).

We found that the distribution of occurrence rate was separated into three groups: 1999–2001, 2002–2018, and 2019 (Fig. 2a, Table 1). The observational year and month of the dusk-side IHFAC types (which are consistent with the Fukushima model or not) are summarized in Table 1. The periods of 1999–2001 and 2012 correspond to the maximum phase of solar cycle in SC23 and SC24, respectively. In these years, the dusk-side IHFAC (bins in blue color, as shown in Fig. 2a), which disagrees with the Fukushima model, had high occurrence rates around not only equinoxes but also around the June solstice. The opposite pattern was found in the year of 2019, which corresponds to the minimum phase of solar cycle SC24. The solar activity in SC24 period was lower than in SC23 (McComas et al. 2013). The F10.7 Flux value during solar maximum phases was larger in SC23 than that in SC24, which may be related to the longer duration of the lower occurrence rate of the dusk-side IHFAC polarity of the Fukushima model type in SC23. The dusk-side IHFAC variations were more related with F10.7 variability, in comparison with the dawn and noon sectors (Fig. 4d–e). Especially, the dusk-side ΔD increased during the declining phase of solar cycle (Figs. 3d and 4b).

As mentioned above in the introduction, other previous studies involving the solar cycle discussion have used the period less than solar cycle period (11 years) (e.g., Park et al. 2011; Owolabi et al. 2018; Lühr et al. 2019). In addition, they have not examined the time-series data of IHFACs in terms of the long-term variation analysis. In the present paper, we used 22-year long-term ΔD data and newly showed the above-mentioned findings as shown in Fig. 4a. In order to better determine the generation mechanism of dusk-side IHFACs from the observational data, we need to investigate the relationship between ΔD and various proxies of magnetospheric disturbances such as Dst and SymH indexes. This point should be done in future work.

Table 1 Year and month of the dusk-side IHFAC suggested by the Fukushima model

Periods	Fukushima model type	Non-Fukushima model type
1999–2001	December solstice	March–November
2002–2018	June/December solstices	March/September equinoxes
2019	June solstice	October–April

Conclusion

We investigated the occurrence rate of the dusk-side IHFAC polarity as suggested by Fukushima's model and examined the solar cycle dependence of IHFACs by using the equatorial ΔD variations at Davao with 1-h time resolution data from August 1998 to July 2020. We found that there were seasonal dependences of the appearance of the dusk-side IHFAC of the Fukushima model type (the same IHFAC polarity between the noon and dusk sectors). The polarities of dawn-side and noontime IHFACs agreed with the Fukushima model irrespective of season: the IHFACs during solstices flow from the summer hemisphere to the winter hemisphere in the dawn sector and from the winter hemisphere to the summer hemisphere around the noon sector (Figs. 1 and 2). The occurrence rate of the dusk-side IHFAC of the Fukushima model type was high around June and December solstices. In contrast, the dusk-side IHFACs, which are inconsistent with the Fukushima model type, dominated from the September to November months and occurred at slightly rates around the March equinox (Fig. 2, Table 1). The remarkable solar cycle dependence of IHFACs was exhibited in the dusk sector. Especially, large IHFACs flowed in the dusk sector during the declining phase of the solar cycle. It is also clear that the noontime and dusk-side IHFACs polarities reversed at the different intersection months. Seasonal variations of ΔD showed asymmetry in both dawn and noon sectors. In contrast, the seasonal dusk-side ΔD variations were symmetric. In order to conclude the generation and modulation mechanisms of the dusk-side IHFAC, we need to conduct further comparative analysis between the long-term development and dynamics of global current systems from polar to middle and low latitudes and the IHFAC excitation pattern.

Abbreviations

CHAMP: Challenging Minisatellite Payload; ICSWSE: International Center for Space Weather Science and Education; FACs: Field-aligned currents; IHFAC: Inter-hemispheric field-aligned current; LT: Local time; MAGDAS/CPMN: MAGnetic Data Acquisition System/Circum-pan Pacific Magnetometer Network Data; Sq: Solar quiet; SC: Solar cycle.

Acknowledgements

Special thanks to Daniel J. McNamara and Quirino M. Sugon Jr., Ateneo de Manila University, for their time and dedication to collecting of the magnetometer data at Davao observatory of MAGDAS network.

Authors' contributions

MR and AF analyzed the data and wrote the manuscript. AF and AY designed the current research and interpreted the data analysis results. CJ gave suggestions for improvement. All authors read and approved the final manuscript.

Funding

This work is financially supported by National Research Council (NRC) of Sri Lanka (16–098). The MAGDAS observation is financially supported by Japan Society for the Promotion of Science (JSPS) as Grant-in-Aid for Overseas Scientific Survey (15253005, 18253005). AF was supported by the JSPS KAKENHI Grant (17J40136, 19K03956). AY was supported by JSPS KAKENHI Grant (19K03956, 15H05815, JP20H01961).

Availability of data and materials

The original data used in this study are publicly available as follows. The ground-based magnetometer data at Davao station of MAGDAS/CPMN are provided by ICSWSE, Kyushu University (http://data.icswse.kyushu-u.ac.jp). The F10.7 and *Dst* indices are provided by the OMNIWeb service of the Space Physics Data Facility at the Goddard Space Flight Center (http://omniweb.gsfc.nasa.gov/). The original source of *Dst* index is WDC geomagnetism Kyoto (https://doi.org/10.17593/14515-74000).

Declarations

Ethics approval and consent to participate

Not applicable.

Consent for publication

Not applicable.

Competing interests

The authors declare that they have no conflict of interest.

Author details

[1]Astronomy and Space Science Unit, Department of Physics, University of Colombo, Colombo, 00300, Sri Lanka. [2]Faculty of Computer Science and Systems Engineering, Kyushu Institute of Technology, 680-4, Kawazu, Iizuka, Fukuoka 820-8502, Japan. [3]International Center for Space Weather Science and Education (ICSWSE), Kyushu University, 744, Motooka, Nishi-ku, Fukuoka 819-0395, Japan.

Received: 1 January 2021 Accepted: 12 July 2021
Published online: 21 July 2021

References

Abidin ZZ, Jusoh MH, Abbas M, Bolaji OS, Yoshikawa A (2019) Features of the inter-hemispheric field-aligned current system over Malaysia ionosphere. J Atmos Solar Terr Phys. https://doi.org/10.1016/j.jastp.2018.01.012

Bolaji OS, Rabiu AB, Oyeyemi EO, Yumoto K (2012) Climatology of the inter-hemispheric field-aligned currents system over the Nigeria ionosphere. J Atmos Solar Terr Phys 89:144–153. https://doi.org/10.1016/j.jastp.2012.07.008

Borovsky JE, Denton MH (2006) Differences between CME-driven storms and CIR-driven storms. J Geophys Res. https://doi.org/10.1029/2005ja011447

Christiansen F, Papitashvili VO, Neubert T (2002) Seasonal variations of high-latitude field-aligned currents inferred from Ørsted and Magsat observations. J Geophys Res. https://doi.org/10.1029/2001JA900104

Echer E, Gonzalez WD, Tsurutani BT, Gonzalez ALC (2008) Interplanetary conditions causing intense geomagnetic storms (Dst ≤ -100 nT) during solar cycle 23 (1996–2006). J Geophys Res. https://doi.org/10.1029/2007ja012744

Edwards TR, Weimer DR, Tobiska WK, Olsen N (2017) Field-aligned current response to solar indices. J Geophys Res 122:5798–5815. https://doi.org/10.1002/2016JA023563

Fambitakoye O, Mayaud PN (1976) Equatorial electrojet and regular daily variation SR—I. A determination of the equatorial electrojet parameters. J Atmos Solar Terr Phys 38(1):1–17. https://doi.org/10.1016/0021-9169(76)90188-4

Fathy A, Ghamry E, Arora K (2019) Mid and low-latitudinal ionospheric field-aligned currents derived from the Swarm satellite constellation and their variations with local time, longitude, and season. Adv Space Res 64:1600–1614

Fujimoto A, Uozumi T, Abe S, Matsushita H, Imajo S, Ishitsuka JK, Yoshikawa A (2016) Long-term EEJ variations by using the improved EE-index. Sun Geosph 11(1):37–47

Fukushima N (1979) Electric potential difference between conjugate points in middle latitudes caused by asymmetric dynamo in the ionosphere. J Geomagn Geoelectr 31:401–409
Fukushima N (1994) Some topics and historical episodes in geomagnetism and aeronomy. J Geophys Res 99(A10):19113–19142
Green DL, Waters CL, Anderson BJ, Korth H (2009) Seasonal and interplanetary magnetic field dependence of the field-aligned currents for both Northern and Southern Hemispheres. Ann Geophys 27:1701–1715. https://doi.org/10.5194/angeo-27-1701-2009
King J, Papitashvili N (2005) Solar wind spatial scales in and comparisons of hourly Wind and ACE plasma and magnetic field data. J Geophys Res. https://doi.org/10.1029/2004JA010649
Lühr H, Kervalishvili G, Michaelis I, Rauberg J, Ritter P, Park J, Merayo JMG, Brauer P (2015) The interhemispheric and F region dynamo currents revisited with the Swarm constellation. Geophys Res Lett 42:3069–3075. https://doi.org/10.1002/2015GL063662
Lühr H, Kervalishvili GN, Stolle C, Rauberg J, Michaelis I (2019) Average characteristics of low-latitude interhemispheric and F region dynamo currents deduced from the swarm satellite constellation. J Geophys Res Space Phys 124:10631–10644
Maeda H (1974) Field-aligned current induced by asymmetric dynamo action in the ionosphere. J Atmos Terr Phys 36:1395–1401
McComas DJ, Angold N, Elliott HA, Livadiotis G, Schwadron NA, Skoug RM, Smith CW (2013) Weakest solar wind of the space age and the current "mini" solar maximum. Astrophys J. https://doi.org/10.1088/0004-637x/779/1/2
NASA (2020) Solar Cycle 25 Is Here. NASA, NOAA Scientists Explain What That Means. https://www.nasa.gov/press-release/solar-cycle-25-is-here-nasa-noaa-scientists-explain-what-that-means/. Accessed 20 Dec 2020
Nose M, Iyemori T, Sugiura M, Kamei T (2015) Geomagnetic Dst index. World Data Cent Geomagnetism Kyoto. https://doi.org/10.17593/14515-74000
Olsen N (1997) Ionospheric F region currents at middle and low latitudes estimated from Magsat data. J Geophys Res 102:4563–4576
Owolabi OP, Bolaji OS, Adeniyi JO, Oyeyemi EO, Rabiu AB, Habarulema JB (2018) Excursions of interhemispheric field-aligned currents in Africa. J Geophys Res Space Phys 123:6042–6053
Park J, Lühr H, Min K (2011) Climatology of the inter-hemispheric field-aligned current system in the equatorial ionosphere as observed by CHAMP. Ann Geophys 29:573–582. https://doi.org/10.5194/angeo-29-573-2011
Park J, Stolle C, Yamazaki Y, Rauberg J, Michaelis I, Olsen N (2020a) Diagnosing low-/mid-latitude ionospheric currents using platform magnetometers: CryoSat-2 and GRACE-FO. Earth Planets Space. https://doi.org/10.1186/s40623-020-01274-3
Park J, Yamazaki Y, Lühr H (2020b) Latitude dependence of interhemispheric field-aligned currents (IHFACs) as observed by the swarm constellation. J Geophys Res Space Phys. https://doi.org/10.1029/2019JA027694
Richardson IG, Cliver EW, Cane HV (2001) Sources of geomagnetic storms for solar minimum and maximum conditions during 1972–2000. Geophys Res Lett 28(13):2569–2572. https://doi.org/10.1029/2001gl013052
Ridley AJ (2007) Effects of seasonal changes in the ionospheric conductances on magnetospheric field-aligned currents. Geophys Res Lett 34:L05101. https://doi.org/10.1029/2006GL028444
Schieldge JP, Venkateswaran SV, Richmond AD (1973) The ionospheric dynamo and equatorial magnetic variations. J Atmos Terr Phys 35(6):1045–1061. https://doi.org/10.1016/0021-9169(73)90004-4
Shinbori A, Koyama Y, Nosé M, Hori T, Otsuka Y (2017) Characteristics of seasonal variation and solar activity dependence of the geomagnetic solar quiet daily variation. J Geophys Res Space Physics 122:10796–10810
SPDF–OMNIWeb Service (2020) SPDF–OMNIWeb Service - NASA. https://omniweb.gsfc.nasa.gov/form/dx1.html. Accessed 10 Aug 2020
Stening RJ (1977) Field-aligned currents driven by the ionospheric dynamo. J Atmos Terr Phys 39:933–937
Takeda M (1982) Three dimensional ionospheric currents and field aligned currents generated by asymmetrical dynamo action in the ionosphere. J Atmos Terr Phys 44(2):187–193. https://doi.org/10.1016/0021-9169(82)90122-2
Takeda M (1990) Geomagnetic field variation and the equivalent current system generated by an ionospheric dynamo at the solstice. J Atmos Terr Phys 52(1):59–67
Tomás AT, Lühr H, Rother M (2009) Mid-latitude solar eclipses and their influence on ionospheric current systems. Ann Geophys 27(12):4449–4461. https://doi.org/10.5194/angeo-27-4449-2009
Van Sabben D (1964) North-South asymmetry of S_q. J Atmos Terr Phys 26:1187–1195. https://doi.org/10.1016/0021-9169(64)90127-8
Van Sabben D (1966) Magnetospheric currents, associated with the N–S asymmetry of Sq. J Atmos Terr Phys 28:965–982. https://doi.org/10.1016/S0021-9169(17)30026-0
Van Sabben D (1969) The computation of magnetospheric currents, caused by dynamo action in the ionosphere. J Atmos Terr Phys 31:469–474. https://doi.org/10.1016/0021-9169(69)90072-5
Van Sabben D (1970) Solstical Sq-currents through the magnetosphere. J Atmos Terr Phys 32:1331–1336. https://doi.org/10.1016/0021-9169(70)90064-4
Webb DF (1995) Solar and geomagnetic disturbances during the declining phase of recent solar cycles. Adv Space Res 16(9):57–69. https://doi.org/10.1016/0273-1177(95)00315-6
Yamashita S, Iyemori T (2002) Seasonal and local time dependences of the interhemispheric field-aligned currents deduced from the Ørsted satellite and the ground geomagnetic observations. J Geophys Res. https://doi.org/10.1029/2002JA009414
Yamazaki Y, Maute A (2017) Sq and EEJ—a review on the daily variation of the geomagnetic field caused by ionospheric dynamo currents. Space Sci Rev 206(1–4):299–405. https://doi.org/10.1007/s11214-016-0282-z
Yamazaki Y, Yumoto K, Cardinal MG, Fraser BJ, Hattori P, Kakinami Y, Liu JY, Lynn KJW, Marshall R, McNamara D, Nagatsuma T, Nikiforov VM, Otadoy RE, Ruhimat M, Shevtsov BM, Shiokawa K, Abe S, Uozumi T, Yoshikawa A (2011) An empirical model of the quiet daily geomagnetic field variation. J Geophys Res. https://doi.org/10.1029/2011ja016487
Yumoto K, 210MM Magnetic Observation Group (1996) The STEP 210 magnetic meridian network project. J Geomag Geoelectr 48(11):1297–1310
Yumoto K, CPMN Group (2001) Characteristics of Pi 2 magnetic pulsations observed at the CPMN stations: a review of the STEP results. Earth Planets Space 53:981–992. https://doi.org/10.1186/BF03351695
Yumoto K, MAGDAS Group (2007) Space weather activities at SERC for IHY: MAGDAS. Bull Astr Soc India 35(4):511–522
Yumoto K, MAGDAS Group (2006) MAGDAS project and its application for space weather, Solar Influence on the Heliosphere and Earth's Environment: Recent Progress and Prospects, Edited by N. Gopalswamy and A. Bhattacharyya. p 309–405.

Publisher's Note